Atomic-Scale Structural Investigations on the Nucleation of Cubic Boron Nitride from Amorphous Boron Nitride under High Pressures and Temperatures

J. Y. Huang* and Yuntian T. Zhu

Los Alamos National Laboratory, Materials Science & Technology Division, MS G755, Los Alamos, New Mexico 87545

Received November 19, 2001. Revised Manuscript Received January 30, 2002

By controlling the microstructure of the starting materials, i.e., by ball-milling a commercial hexagonal boron nitride (h-BN) to an amorphous boron nitride (a-BN), the subsequent high-pressure and high-temperature (HP−HT) induced phase transformation has been significantly facilitated. Namely, cubic boron nitride (c-BN) forms at 900 °C and achieves accomplishment at 1350 °C under 7.7 GPa, which are significantly less-extreme conditions than that of crystalline h-BN under similar HP−HT treatments. High-resolution transmission electron microscopy (HRTEM) and electron energy loss spectroscopy (EELS) clarified the nucleation mechanism at an atomic scale. It demonstrated that the c-BN phase nucleates directly from the sp^3-hybridized amorphous matrix, which is originally induced by ball-milling and is therefore responsible for the reduced HP−HT conditions. This c-BN nucleation mechanism is completely different from the so-called diffusionless "puckering" mechanism involved in the HP−HT experiments starting from crystalline h-BN but very similar to one of the proposed mechanisms involved in the chemical vapor deposition (CVD) of diamond and c-BN. It turns out that the present experimental results provide not only a less-extreme way to synthesize nanocrystalline c-BN material but also key clues to the understanding of the nucleation mechanisms involved in the CVD diamond or c-BN, which are still under controversy.

Introduction

The fascinating properties of cubic boron nitride (c-BN) such as the extreme hardness, high melting point, and wide band gap have motivated many experimental and theoretical studies on this material. In contrast to diamond, c-BN is not dissolved in iron and steel, and based upon this premise, studies to utilize this material as a coating of high duty tools are in progress.

There are two sp^2-bonded graphite-like—and two sp^3-bonded diamond-like—polymorphic modifications of boron nitride. The former corresponds to hexagonal (h-BN) and rhombohedral (r-BN) BN and the latter to cubic zinc blende (c-BN) and hexagonal wurzite-type (w-BN) BN. In addition, there are two other disordered BN phases which are called turbostratic BN (t-BN)[1] and amorphous BN (a-BN). In t-BN, the stacking of the sp^2 layers is random, and the layers are rotated randomly along the *c*-axis. a-BN is characterized by an atomic level structural disorder. Bulk c-BN is usually synthesized by applying high pressure and high temperature (HP−HT) to induce the so-called hexagonal-to-cubic transformation. Structurally, direct compressing along the *c*-axis of h-BN produces w-BN (a so-called "puckering" mechanism[2]), and w-BN transforms to c-BN via a dislocation mechanism. The definite orientation relationships, i.e., $(0002)_h//(0002)_w//(111)_c$, $[11\bar{2}0]_h//[11\bar{2}0]_w//[\bar{1}10]_c$,[3,4] being present among the h-, w- and c-BN phases are direct verifications of such a mechanism. A complete conversion to c-BN in the puckering mechanism requires a pressure higher than 8.5 GPa and a temperature higher than 2000 °C,[5−7] which are very crucial experimental conditions. Therefore, since the first successful synthesis of c-BN, efforts have been continued in searching for new synthesis means so as to get c-BN at less extreme conditions.[8−15] By using a catalyst effect[8−12] or by controlling the grain size or crystallinity of the starting h-BN,[13−15] the synthesis pressure and temperature are reduced appreciably. By using a-BN as a starting material,[14] it was found that

* Corresponding author: Tel 505-665-0835, Fax 505-667-2264, e-mail jyhuang@lanl.gov.

(1) Thomas, J., Jr.; Weston, N. E.; O'Connor, T. E. *J. Am. Chem. Soc.* **1963**, *84*, 4619.
(2) Kurdyumov, A. V.; Britun, V. F.; Petrusha, I. A. *Diamond Relat. Mater.* **1996**, *5*, 1225.
(3) Horiuchi, S.; Huang, J. Y.; He, L. L.; Mao, J. F.; Taniguchi, T. *Philos. Mag. A* **1998**, *78*, 1065.
(4) Huang, J. Y.; Zhu, Y. T. *Defects Diffusion Forum* **2000**, *186−187*, 1.
(5) Bundy, F. P.; Wentorf, R. H., Jr. *J. Chem. Phys.* **1963**, *38*, 1144.
(6) Corrigan, F. R.; Bundy, F. P. *J. Chem. Phys.* **197**5, *63*, 3812.
(7) Wentorf, R. H., Jr. *J. Chem. Phys.* **1957**, *26*, 956.
(8) DeVries, R. C.; Fleischer, J. F. *J. Cryst. Growth* **1972**, *13/14*, 88.
(9) Endo, T.; Fukunaga, O.; Iwata, M. *J. Mater. Sci.* **1979**, *14*, 1375.
(10) Kobayashi, T. *J. Chem. Phys.* **1979**, *70*, 5898.
(11) Choi, J. Y.; Kang, S. J. L.; Fukunaga, O.; Park, J. K.; Eun, K. Y. *J. Am. Ceram. Soc.* **1993**, *76*, 2525.
(12) Singh, B. P.; Nover, G.; Will, G. *J. Cryst. Growth* **1995**, *152*, 143.
(13) Wakatsuki, M.; Ichinose, K.; Aoki, T. *Mater. Res. Bull.* **1972**, *7*, 999.
(14) Sumiya, H.; Iseki, T.; Onodera, A. *Mater. Res. Bull.* **1983**, *18*, 1203.
(15) Gladkaya, I. S.; Kremkova, G. N.; Slesarev, V. N. *J. Less-Common Met.* **1986**, *117*, 241.

10.1021/cm0109645 CCC: $22.00
Published on Web 03/06/2002

a small amount of c-BN phase arises at pressures higher than 6 GPa and temperatures greater than 800 °C with a small amount of w-BN also present. It was also reported that t-BN undergoes a direct transformation to c-BN at 6 GPa and 1000 °C, and w-BN was claimed to be not present in the products.[15] There still exist discrepancies in the phase transformation routes in direct transformation of disordered BN under HP−HT conditions. In addition, the underlying mechanisms involved in both the catalyst effect and the grain size or crystallinity effect are unclear.

In this paper, the ball-milling (BM) technique was employed to control the crystallinity of the starting h-BN powders so as to investigate the mechano-chemical effect on the phase transformation of h-BN under HP−HT conditions. We demonstrate that a mechano-chemical effect induced by BM can affect the hexagonal-to-cubic transformation significantly, and the HP−HT conditions are reduced appreciably. The underlying mechanism responsible for this significantly facilitated phase transformation was clarified by atomic scale structural investigations including high-resolution transmission electron microscopy (HRTEM) and electron energy loss spectroscopy (EELS).

Experimental Section

Commercial h-BN powders with high crystallinity and large grain size (millimeter scale) were milled in a planetary-type ball mill under the protection of a nitrogen atmosphere. Possible contamination from the milling tools was analyzed by inductively coupled plasma atomic emission spectroscopy (ICP-AES), which showed that there was essentially no W, C, or Co contamination (less than 50 ppm). The milled powders were then subjected to HP−HT conditions of 7.7 GPa and 800−1600 °C for 15 min. The phases and microstructures of the retrieved samples were characterized by X-ray diffraction (XRD), HRTEM, and EELS. HRTEM observation was performed in a high-voltage electron microscope (model H-1500) operated at an accelerating voltage of 800 kV with a point resolution of 0.14 nm. EELS experiments were carried out in a HF-3000 field emission gun (FEG) TEM equipped with a Gatan 666 parallel electron energy-loss spectrometer. The operating voltage was 300 kV. The probe diameter was about 2 nm, and the energy resolution was about 1.5−2 eV (full-width at half-maximum of the zero-loss peak). To acquire EELS, the typical photodiode readout times were 10−30 s for the core-loss and 25 ms for the valence-loss spectra. Beam convergence and collection angles were limited by microscope apertures to be about 10 and 20 mrad, respectively. Corrections for the photodiode dark current and fixed readout pattern were made to the data. All the core-loss spectra shown in the paper have had a smooth background subtracted from beneath the boron edge. The background was modeled by a power-law curve, fitted in the preedge region. TEM samples were prepared both by suspending the powders on carbon-coated microgrids or by a normal sample preparation method involving mechanical grinding, dimpling, and subsequent ion beam milling.

Results

Phase Determination by XRD. Figure 1 shows the XRD patterns of the starting h-BN powders and the milled one. The sharp diffraction peaks in the starting material (Figure 1a) are replaced by two broad amorphous-like haloes in the milled powders (Figure 1b), indicating that an amorphous-like phase is produced by BM. This is further confirmed by HRTEM investigations, which showed that the end product is essentially a mixture of a nanocrystalline and an amorphous phase (Figure 2). The grain sizes of the nanocrystals are less than 3 nm, and their stacking is entirely turbostratic. The electron diffraction pattern (EDP) also exhibits amorphous haloes (Figure 2, inset), being consistent with the XRD result. The XRD patterns of the h-BN and the a-BN samples after HP−HT treatment are depicted in Figures 3 and 4, respectively. It is seen from Figure 3 that a small amount of c-BN and w-BN phases appear at 1450 °C, but the h-BN phase only partly transforms to the c-BN phase even at a temperature as high as 1600 °C. In contrast, it is seen from Figure 4 that the majority of the a-BN and h-BN transform to the c-BN phase at 1000 °C, and an almost single c-BN phase is produced at 1350 °C.

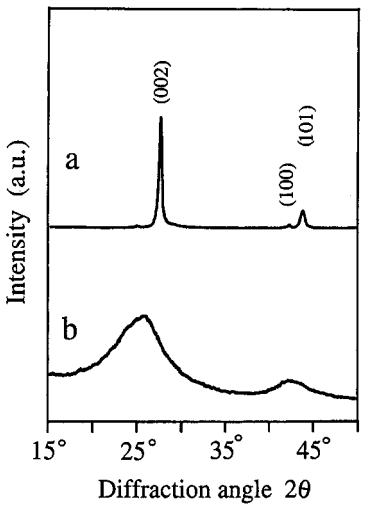

Figure 1. XRD patterns of the starting h-BN (a) and h-BN after 33 h of ball-milling (b).

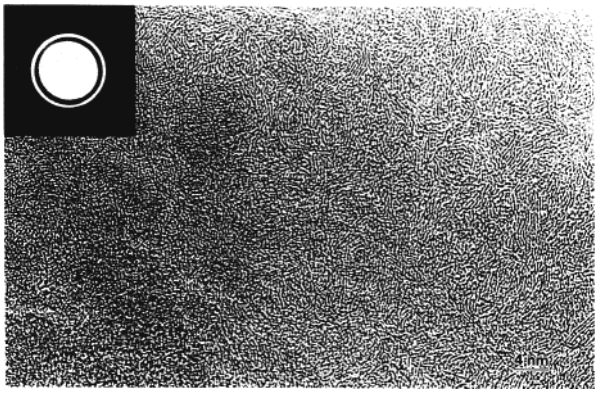

Figure 2. A HRTEM image with the corresponding EDP as inset from an a-BN sample synthesized by ball-milling of h-BN for 33 h.

Microstructure and Phase Characteristics Revealed by HRTEM. The above XRD results are further confirmed by HRTEM investigations. Figure 5 shows an HRTEM image from an a-BN sample pressed under 900 °C at 7.7 GPa. In this picture, besides the h-BN phase which is crystallized from the a-BN phase, surprisingly, the c-BN phase is readily detected at such a low temperature, even though one cannot identify it clearly from the XRD as shown in Figure 4, owing to the broadening and overlapping of the c-BN (111) and the h-BN {10} reflections. The identification of c-BN phase is based on the two-dimensional lattice images

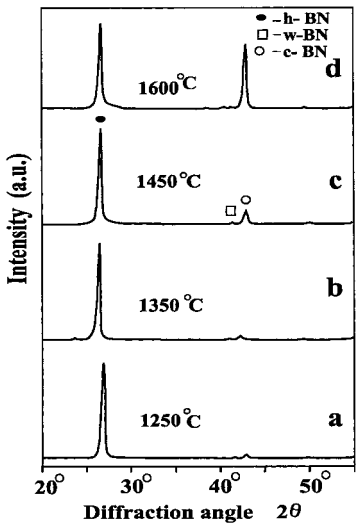

Figure 3. XRD patterns of h-BN after pressing for 15 min at 7.7 GPa and at various temperatures as shown in the figure.

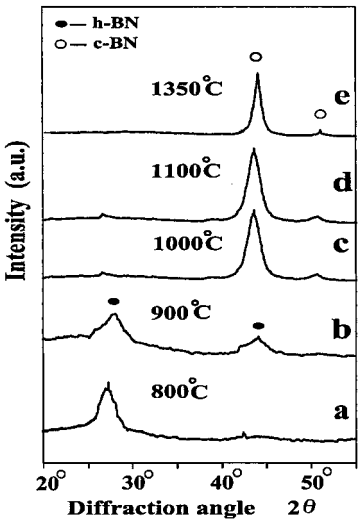

Figure 4. XRD patterns of a-BN after pressing for 15 min at 7.7 GPa and at various temperatures as shown in the figure.

which enable one to determine the two sets of (111) planes and the included angles between them clearly. The c-BN grains are less than 3 nm in size, and they are nucleated from the amorphous matrix directly. It is interesting to note that twinning, a typical defect found in chemical vapor deposition (CVD) diamond[16] or CVD c-BN,[17] readily takes place even at the nucleation stage. The grain size of the h-BN phase is less than 5 nm, and various lattice defects such as dislocations and shearing of the lattice planes can be found. Previous investigations showed that any imperfections in the h-BN phase favor the c-BN formation,[3,4] which is also consistent with recent atomic-scale structural characterization results on the nucleation process of c-BN deposited from the vapor phase.[18] The c-BN grains grow at the expense of the surrounding h-BN and a-BN phases with an increasing temperature. Figure 6a,b depicts HRTEM images of an a-BN sample after HP−

(16) Luyten, W.; Tendeloo, G. van; Amelinckx, S. *Philos. Mag. A* **1992**, *66*, 899.
(17) Zhou, D. S.; Chen, C. L.; Michell, T. E.; Hackenberger, L. B.; Messier, R. *Philos. Mag. Lett.* **1995**, *72*, 163.
(18) Yamada-Takamura, Y.; Tsuda, O.; Ichinose, H.; Yoshida, T. *Phys. Rev. B* **1999**, *59*, 10351.

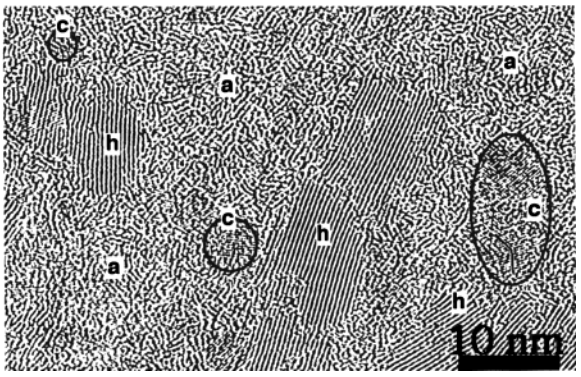

Figure 5. A HRTEM image of an a-BN sample after pressing for 15 min at 7.7 GPa and at 900 °C, showing the nucleation of c-BN phase from the amorphous matrix or from the edge of small h-BN grains; "a", "h", and "c" represent amorphous BN, h-BN, and c-BN phases, respectively. The three circled c-BN grains show near [110] orientation lattice images and therefore can be identified clearly. The white-edged black lines denote twining in a c-BN grain.

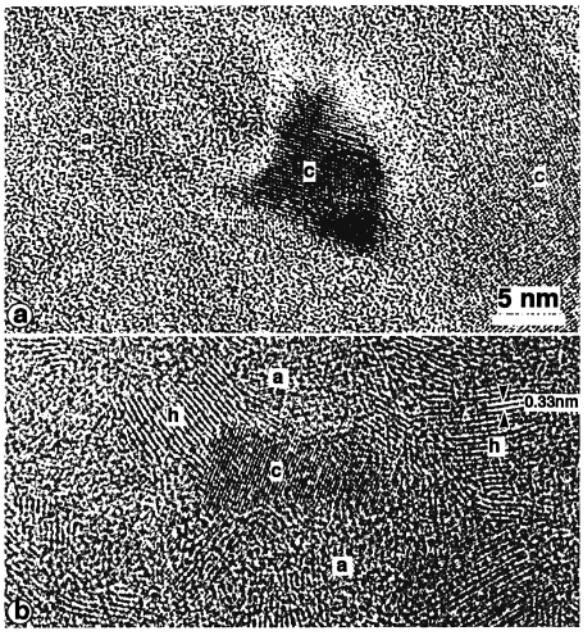

Figure 6. HRTEM images from an a-BN sample after pressing for 15 min at 7.7 GPa and at 1000 °C, showing the coexistence of a-BN and c-BN (a), and the coexistence of h-BN, a-BN, and c-BN (b). "h", "a", and "c" denote h-BN, the amorphous, and cubic phase, respectively.

HT treatment of 7.7 GPa and 1000 °C, showing c-BN grains arising from the amorphous matrix (Figure 6a) or from the edge of h-BN grains (Figure 6b). It should be mentioned that the a-BN phase was detected in all the samples after HP−HT conditions of 7.7 GPa and temperatures less than 1000 °C. The bonding nature of the a-BN phase present at different conditions was analyzed by EELS, and details will be described later. We will show that the presence of the a-BN phase is significant to the c-BN nucleation. At 1350 °C, TEM observations showed that a homogeneous tetrahedral-shaped nanocrystalline c-BN phase is synthesized, and typical TEM micrographs are displayed in Figure 7. From Figure 7a,b, it is seen that the grain size of the c-BN grains is about 30 nm; the grain boundaries are slightly strained and are thus clearly visible. The corresponding electron diffraction pattern in Figure 7c

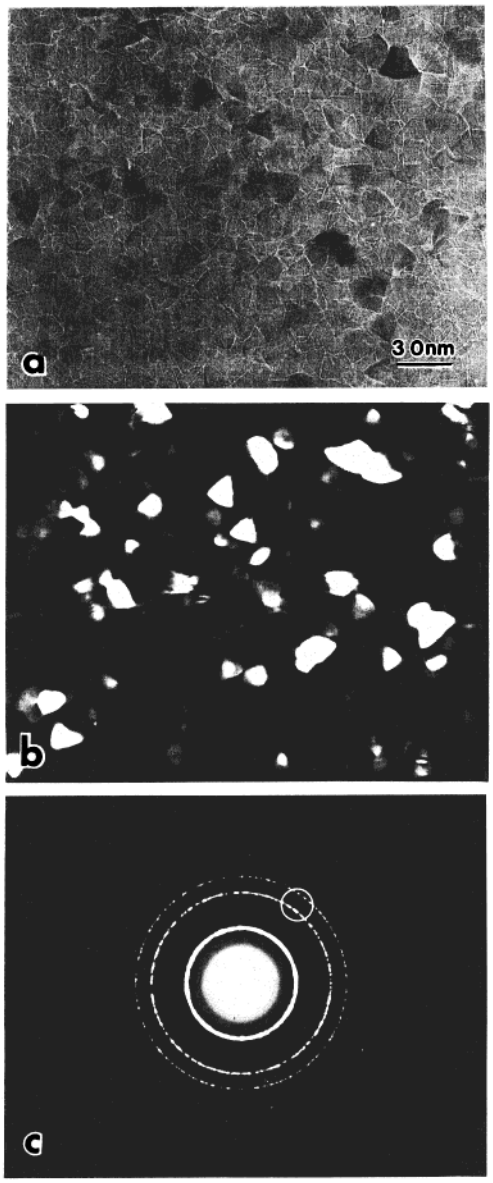

Figure 7. TEM micrographs from an a-BN sample after pressing for 15 min at 7.7 GPa and at 1350 °C: (a) bright-field image; (b) dark-field image; (c) corresponding electron diffraction pattern. Circle marks the diffraction used for the dark-field image in (b).

can effectively be indexed as that of c-BN, which further confirms the XRD result (Figure 4e). It should be mentioned that HRTEM investigations revealed clearly that w-BN is not formed in the product, which clarifies the debate in previous experiments.[12−15]

In summary, our results showed that, starting from an a-BN fabricated by BM, cubic phase starts to appear at 900 °C and achieve accomplishment at 1350 °C under 7.7 GPa. The c-BN grains nucleate directly from the amorphous matrix and grow via a diffusional process.

Discussion

EELS Evaluation of the Bonding State of Different BN Materials. The above nucleation mechanism is significantly different from the diffusionless puckering mechanism operated in the HP−HT experimentals carried out with high-crystallinity h-BN powders as a staring material,[3,4] in which c-BN nucleation

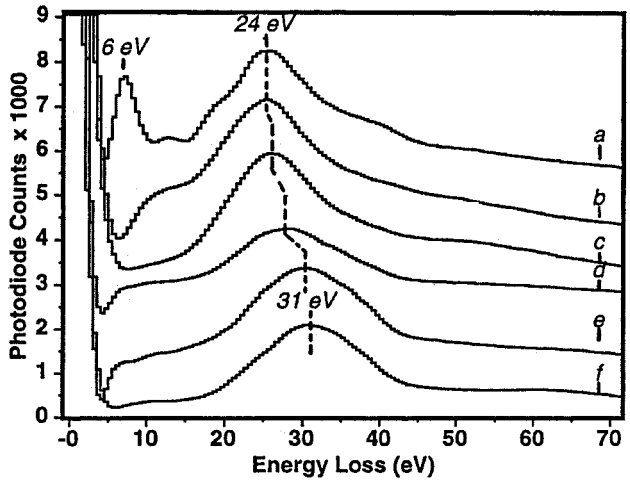

Figure 8. Low-energy loss spectra from (a) polycrystalline h-BN grains, (b) a-BN prepared by ball-milling, (c) amorphous regions in the a-BN after pressing at 7.7 GPa and 900 °C, (d) amorphous regions in the a-BN sample after pressing at 7.7 GPa and 1000 °C, (e) amorphous regions around c-BN grains in the a-BN sample after pressing at 7.7 GPa and 1000 °C, and (f) c-BN grains. Note that the peak position of the bulk plasmon mode varies with the sample types.

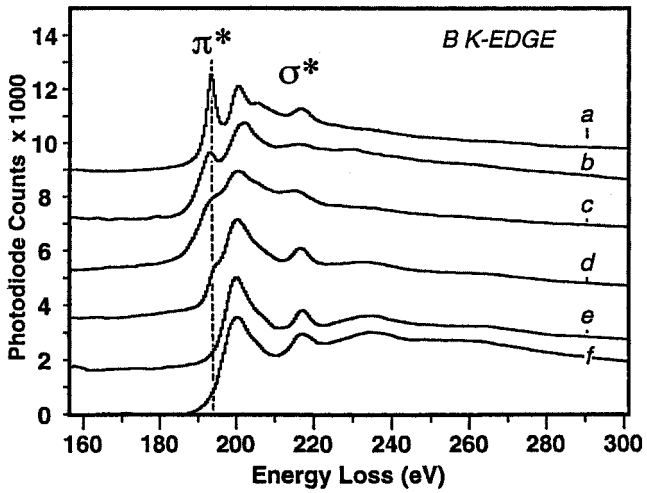

Figure 9. EELS spectra showing B−K absorption edges of (a) polycrystalline h-BN grains, (b) a-BN prepared by ball-milling, (c) amorphous regions in an a-BN sample after pressing at 7.7 GPa and 900 °C, (d) amorphous regions in an a-BN sample after pressing at 7.7 GPa and 1000 °C, (e) amorphous regions around c-BN grains in an a-BN sample after pressing at 7.7 GPa and 1000 °C, and (f) c-BN grains.

always proceeds through a w-BN intermediate, and definite orientation relationships exist among h-, w-, and c-BN. w-BN forms from h-BN by direct compress along the *c*-axis while c-BN forms from w-BN by a dislocation glide mechanism. The starting temperature for c-BN formation is 1450 °C while a complete conversion needs a temperature as high as 2000 °C, which are appreciably higher than that starting from the amorphous materials.

The above comparison shows a clear mechano-chemical effect on the HP−HT synthesis of c-BN. To get a further insight into the mechano-chemical effect, we investigated the bonding state of the various BN phases by the EELS technique, and typical EELS spectra obtained are shown in Figures 8 and 9. Namely, a series of plasmon-loss and of core-loss spectra obtained from

the polycrystalline h-BN (a), ball-milled a-BN (b), a-BN in samples after HP−HT conditions of 7.7 GPa and 900 °C (c), 1000 °C (d), a-BN around c-BN (e), and nanocrystalline c-BN (f) are shown in Figures 8 and 9. The most notable feature of the low-loss spectra shown in Figure 8 is that the peak positions of the bulk plasmon mode are different, and they shift from 24 eV of the polycrystalline h-BN phase (a) to 31 eV of the c-BN phase (f), indicating an increase of the density in the corresponding materials. The EELS spectrum from h-BN (Figure 8a) has a peak at about 6 eV, corresponding to transition between π and π^* states. This interband transition peak was not observed in the a-BN sample (Figure 8b). The π to π^* transition peak in amorphous carbon (a-C) is much weaker and broader than that in hexagonal graphite due to the existence of sp^3 hybridization and the poor crystallinity in a-C.[19] The same is true for our a-BN sample. The broad peak and weak intensity make such a peak easily masked by the tail of the elastic peak and thus indiscernible. It should be noted that the relative intensity of the π to π^* transition peak in single-crystal graphite is very sensitive to the beam/specimen orientation as a result of the strong directionality of the π bond.[19] The same is true for our a-BN sample if only a limited number of crystallites are radiated. How to eliminate the orientation effect is described later. In the core-loss spectra shown in Figure 9, the peak in the region from 188 to 196 eV results from excitations of electrons in the ground-state 1s core levels to the vacant π^*-like antibonding states. Excitations to the higher lying σ^* states occur above 190 eV. It is seen that the intensity of the π^* peak and the σ^* peak differs from sample to sample. To a good approximation, the ratio of the integrated areas under the π^* and the σ^* energy windows is proportional to the relative number of π^* and σ^* orbitals, which is 1/3 for 100% sp^2-bonded BN and 0/4 for completely sp^3-bonded BN. If there is a fraction of sp^2-bonded BN, x, it can be estimated using the formula[20,21]

$$[I_{\pi^*}/I_{s\sigma^*}]_u/[I_{\pi^*}/I_{\sigma^*}]_h = 3x/(4 - x) \quad (1)$$

where I_{π^*} is the integrated intensity in the range from 190 to 195 eV, I_{σ^*} is the intensity range from 198 to 208 eV, and the subscripts u and h refer to the ratio determined from a sample with unknown sp^2/sp^3 ratio and h-BN. It is well-known that the I_{π^*}/I_{σ^*} ratio can be changed appreciably with the crystal orientation in graphite-like materials. To eliminate orientation effects, a lot of spectra were collected from small-grained h-BN phase with different orientations and then mathematically average the π^* and the σ^* components over all equally likely orientations. The results of the quantitative analysis of the boron K-edge are summarized as follows. First, there is about 30% sp^3-bonded a-BN in the a-BN sample prepared by BM. Considering there exist a number of dangling bonds which contribute to the intensity of the π^* peak,[22] the real fraction of sp^3-bonded a-BN may even be larger than 30%. Second, the sp^3 fraction in the amorphous phase increases with the rise of pressing temperature, say from 39% at 900 °C to above 50% at 1000 °C, and even completely sp^3-bonded a-BN was found in the a-BN sample pressed at 1000 °C, a typical EELS spectrum of which is shown in Figure 9e. This spectrum was collected from an amorphous area surrounding the c-BN grains as shown in Figure 6a. It is seen that EELS spectrum from such amorphous regions exhibit similar profile to that of c-BN, indicating a sp^3-hybridized a-BN is readily formed. The core-loss spectrum from c-BN (Figure 9f) is reasonably consistent with that obtained by other researchers.[23] The similarity in profile between a-BN (Figure 9e) and c-BN (Figure 9f) is attributed to the fact that the amorphous structure may actually comprise of fine clusters of c-BN. It is difficult to discriminate clearly the fine-grained nanocrytals from amorphous materials even by HRTEM.

From the above HRTEM and EELS results, it is reasonable to propose that the sp^3-hybridized structural units in the a-BN phase obtained by BM act as effective nucleation sites of the c-BN phase in the subsequent HP−HT experiments and thus facilitate the hexagonal-to-cubic transformation.

Catalyst Effect of B_2O_3 or H_2O. However, it is speculated that residual B_2O_3 in the commercial h-BN powders may induce a catalyst effect and therefore facilitated the c-BN synthesis.[11] Others claimed that B_2O_3 does not have a catalytic effect, but NH_3-based substance such as ammonium borate ($NH_4B_5O_5 \cdot 4H_2O$) resulted from the reaction of the starting h-BN with water may act as a flux and thus facilitate the synthesis of c-BN.[10] In our experiments, during the transition of the milled powder to the HP−HT apparatus, the freshly milled powder is so active that it reacts with water in the air immediately and release heat and ammonia gas, as evidenced by the strong ammonia smell in the air and also revealed by the oxygen energy-loss peak in the EELS spectrum of the a-BN sample.[24] Possible reaction involved in this process could be[25] $BN + 3H_2O \rightarrow NH_3 + H_3BO_3$. Further reaction undergone during the HP−HT experiments is unclear. However, according to ref 10, those catalysts that produce ammonia borate with large ammonium content favor the hexagonal-to-cubic transformation. It is interesting to note that both ammonium and water, proving to be effective catalysts, are comprised of highly sp^3-like hybridization structural units, which are speculated to be the effective nucleation sites in CVD diamond.[26,27] It turns out that although the HP−HT and CVD methods appear to be entirely different synthesis routes, i.e., in the former high-pressure and high-temperature are involved while in the latter low pressure normal or less higher temper-

(19) Berger, S. D.; McKenzie, D. R.; Martin, P. J. *Philos. Mag. Lett.* **1988**, *57*, 285.
(20) Cuomo, J. J.; Doyle, J. P.; Bruley, J.; Liu, J. C. *Appl. Phys. Lett.* **1991**, *58*, 466.
(21) Bruley, J.; Williams, D. B.; Cuomo, J. J.; Pappas, D. P. *J. Microsc.* **1995**, *180*, 22.
(22) Muramatsu, W.; Oshima, M.; Kawai, J.; Tadokoro, S.; Adachi, H.; Agui, A.; Shin, S.; Kato, H. *Phys. Rev. Lett.* **1996**, *76*, 3846.
(23) Wibbelt, M.; Kohl, H.; Kohler-Redlich, P. *Phys. Rev. B* **1999**, *59*, 11739.
(24) Huang, J. Y. Unpublished results.
(25) Heslop, R. B.; Robinson, P. L. *Inorganic Chemistry*, 3rd ed.; Elsevier Publishing Co.: Amsterdam, 1967.
(26) Lambrecht, R. L. W.; Lee, C. H.; Segall, B.; Angus, J. C.; Li, Z.; Sunkara, M. *Nature* (*London*) **1993**, *364*, 607.
(27) Yugo, S.; Semoto, K.; Hoshina, K.; Kimura, T.; Nakai, H. *Diamond Relat. Mater.* **1995**, *4*, 903.

ature are usually applied; nevertheless, the underlying nucleation mechanism exhibits common characteristics, namely, a high sp^3 hybridization in the starting materials favors the diamond or c-BN nucleation and twins were found in both cases. As such, the present experimental results may provide not only a less extreme way to synthesize nanocrystalline c-BN but also key clues to understand the nucleation mechanisms involved in the CVD diamond and c-BN, which are still under controversy.

About the sp^3 Bonds in the Ball-Milled a-BN. The origin of the sp^3 hybridization is also a matter of concern. It is suggested that the high pressure induced by BM (2−6 GPa)[28] might be an important factor accounting for the production of sp^3 a-BN. It is possible that this sp^3 a-BN may be transformed from sp^2 a-BN, which may be a manifestation of the same kind of first-order phase transition as that occurred in amorphous ice in which it was reported that there exists a phase transformation from low-density state to high-density state under high pressure.[29] Another explanation comes from the fact that any curvature of the sp^2-bonded hexagonal network in h-BN will induce some degree of sp^3 hybridyzation.[30,31] HRTEM images indeed verify that curvature is a common structure feature of ball-milled BN. In CVD diamond or c-BN, the initial sp^3-hybridized structural units were suggested to be originating from etching of hydrogen along the prismatic planes of graphite[26] or from the compressive stress induced by ion sputtering or other reasons.[27,32−35]

Conclusions

Using an a-BN fabricated by ball-milling as a starting material for the HP−HT experiments, the transformation to c-BN phase has been significantly facilitated. Namely c-BN appears at 900 °C and achieves accomplishment at 1350 °C under 7.7 GPa, which are significantly less-extreme conditions than that of crystalline h-BN under similar HP−HT experiments. HRTEM and EELS provide clear evidence that the c-BN phase nucleates directly from the sp^3 or highly sp^3-like hybridized structural units induced by ball-milling, which is responsible for the reduced HP−HT conditions. The present c-BN nucleation mechanism is completely different from the diffusionless puckering mechanism involved in the HP−HT experiments starting from crystalline h-BN, but very similar to one of the proposed mechanisms involved in the CVD diamond and c-BN. Therefore, the present experimental results provide not only a less-extreme way to synthesize nanocrystalline c-BN material but also key clues to the understanding of the nucleation mechanisms involved in the CVD diamond or c-BN, which remain unclear.

CM0109645

(28) Huang, J. Y.; Wu, Y. K.; Ye, H. Q. *Acta Mater.* **1996**, *44*, 1211.
(29) Mishima, O.; Calvert, L. D.; Whalley, E. *Nature (London)* **1985**, *314*, 76.
(30) Bourgeois, L. N.; Bursill, L. A. *Philos. Mag. A* **1997**, *76*, 753.
(31) Huang, J. Y.; Yasuda, H.; Mori, H. *Chem. Phys. Lett.* **1999**, *303*, 130.
(32) Mckenzie, D. R.; McFall, W. D.; Sainty, W. G.; Davis, C. A.; Collins, R. E. *Diamond Relat. Mater.* **1993**, *2*, 970.
(33) Kester, D. J.; Ailey, K. S.; Lichtenwalner, D. J.; Davis, R. F. *J. Vac. Sci. Technol. A* **1994**, *12*, 3074.
(34) Li, Z.; Wang, L.; Suzuki, T.; Argoitia, A.; Pirouz, P.; Angus, J. C. *J. Appl. Phys.* **1993**, *73*, 711.
(35) Medlin, D. L.; Friedmann, T. A.; Mirkarimi, P. B.; Mills, M. J.; McCarty, K. F. *Phys. Rev. B* **1994**, *50*, 7884.